Chemical Engineering Journal 380 (2020) 122471

Contents lists available at ScienceDirect

Chemical Engineering Journal

journal homepage: www.elsevier.com/locate/cej

A novel phosphorus-containing semi-aromatic polyester toward flame retardancy and enhanced mechanical properties of epoxy resin

Xiao-Feng Liu, Bo-Wen Liu, Xi Luo, De-Ming Guo, Hai-Yi Zhong, Li Chen*, Yu-Zhong Wang*

Collaborative Innovation Center for Eco-Friendly and Fire-Safety Polymeric Materials, National Engineering Laboratory of Eco-Friendly Polymeric Materials (Sichuan), State Key Laboratory of Polymer Materials Engineering, College of Chemistry, Sichuan University, Chengdu 610064, China

HIGHLIGHTS

- P-containing polyester was designed and used as multi-functional modifier for EP.
- The resultant thermosets showed superb flame retardancy and mechanical properties.
- Transparency, T_g and thermal stability of the resultant thermosets were maintained.

ARTICLE INFO

Keywords:
Semi-aromatic polyester
Epoxy resin
Flame retardancy
Toughening

ABSTRACT

Aiming to develop high performance flame-retardant epoxy resin (EP), a novel phosphorus-containing semi-aromatic polyester named poly[4,4′-bis(6-hydroxyhexyloxy)biphenyl 9,10-dihydro-10-[2,3-di(hydroxycarbonyl) propyl]-phosphaphenanthrene-10-oxide] (PBHDDP) was synthesized and employed as a multi-functional additive for EP with simultaneously flame retardation and mechanical enhancement. Appropriate thermodynamic compatibility between PBHDDP and the EP network made no phase separation occurred in the process of curing reaction. Compared with neat EP, the resultant EP thermoset containing barely 2.5 phr (2.44 wt%) of PBHDDP exhibited superior mechanical properties with 20.3% and 149% increase in tensile and impact strengths, respectively. Simultaneously, as increasing the content of PBHDDP, flame retardancy of the thermosets enhanced obviously as evidenced by the elevated anti-ignition and self-extinguishing performance, along with the reduced combustion rate and heat release. Whereas, obvious sacrifice of either transparency, glass transition temperature or thermal stability was absent. The exploration of this novel state-of-art that simultaneously improved the mechanical properties and flame retardancy of EP thermosets at a relatively low content of a single-component multi-functional additive provided a powerful basis for the technologies and potential industrial applications.

1. Introduction

Epoxy resins (EPs) have found a broad range of applications in diverse fields such as aerospace, automobile manufacturing, electrical and electronic devices etc. due to their superior thermal and chemical resistance, excellent mechanical and electrical properties, ease of processing and low cost [1–3]. Though EPs have been used in diverse applications, the intrinsic drawbacks of the final thermosets such as flammability and brittleness restrict their application with stringent requirements [4,5]. Thus, it is essentially imperative to develop EP thermosets with both expected flame retardancy and enhanced mechanical properties, especially high fracture toughness to broaden their applications.

In general, adding flexible thermoplastic polymers, such as aliphatic polyesters can increase the toughness of related thermosets at a relatively high loading level (over 10 wt%), but the strength, elastic modulus, thermal stability and glass transition temperature (T_g) will simultaneously deteriorate in a major way due to high flexibility and inferior thermal stability of the polymers [6,7]. In these toughened EP systems, the fracture toughness enhancement strongly correlates with final two- or multi-phase morphologies in particular, a co-continuous or phase-inverted morphology is always necessary to achieve a desirable improvement [8]. However, on the one hand, fine phase-separated morphology is difficult to control, on the other hand, the phase-separated morphology might lead to some unwanted interfacial effects, such as reducing the capability to form seamless contact with the mould surfaces and reducing dimensional stability of the final products [9]. To address these issues, it is necessary to obtain EP thermosets without

* Corresponding authors.
E-mail addresses: l.chen.scu@gmail.com (L. Chen), yzwang@scu.edu.cn (Y.-Z. Wang).

https://doi.org/10.1016/j.cej.2019.122471
Received 10 May 2019; Received in revised form 18 July 2019; Accepted 9 August 2019
Available online 10 August 2019
1385-8947/

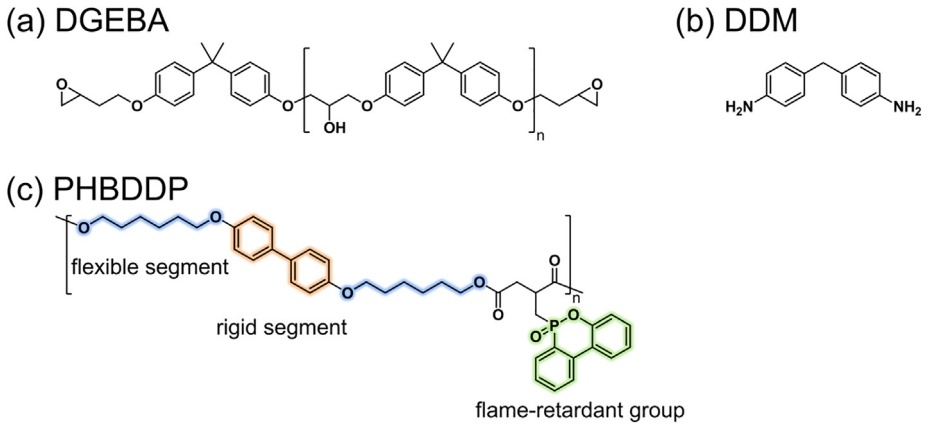

Scheme 1. Chemical structures of the DGEBA-type epoxy resin (a), the curing agent DDM (b) and PHBDDP (c) used in this work.

phase separation to remarkably improve toughness. The major toughening strategies to obtain a no phase-separated morphology fall into three categories:(i) adding flexible curing agents, for example, aliphatic amine [10] and poly(oxypropylene) diamine [11]; (ii) modifying with hyperbranched polymers (HBP) [9]; and (iii) introducing thermoplastic polymers to form interpenetrating (IPN) or semi-interpenetrating polymer networks (semi-IPN) [12,13]. However, for flexible curing agents, the obtained dense and loose network structures inevitably lead to reduced T_g and modulus of the resulting thermosets. For HBP-containing systems, poor control ability restricts their practical application in toughening thermosets [14]. Interestingly, the last category is expected to combine desirable attributes of the two polymer components and seems an effective method for controlling network topology to endow the final thermosets with excellent overall performances without sacrificing other important physical properties, thus to meet versatile requirements for practical application [12]. Unfortunately, poor flame retardancy of the EP thermosets became the dominant drawback, particularly when these flexible components were added into, such situation was getting worse.

Tremendous efforts have been dedicated to preparing flame-retardant EP materials with incorporation of different halogen-free flame retardants [15–17]. Thereinto, organophosphorus additives have received a considerable attention from both industrial and academic circles [18–21]. However, owing to the inferior properties of these phosphorus-containing compounds, numerous existing flame-retardant EP systems are accompanied by dramatic deteriorations in other original properties of the thermoset, especially T_g [22], initial degradation temperature [23,24], and mechanical properties [25,26]. Thus, how to address the contradiction between improving flame retardancy and retaining or even enhancing mechanical properties of EP thermosets is instructive for both academic and industrial fields.

Polymer-type flame retardants, particularly with typical rigid-flexible molecular structures, that possess intrinsic high mechanical properties and flame-retardant efficiency, seems to be an ideal all-purpose additive to afford expected mechanical properties and flame retardancy for the resulting thermosets simultaneously. Perez et al. synthesized a novel phosphorus-containing thermoplastics by introducing 9,10-dihydro-9-oxa-10-phosphaphenantrene-10-oxide (DOPO) as the pendent group of poly(sulfone) (P-PSu) and incorporated it into the amine-cured EP thermosets, which showed somewhat improvements in toughness and flame retardancy, but the increment was limited [27]. Other phosphorus-containing polymers, such as linear polyphosphazene [23], dicarboxyl aromatic polyphosphonate [22], hyperbranched poly(aminomethylphosphine oxide-amine) [28] and hyperbranched poly(urethane-phosphine oxide) [29], can endow the resultant thermosets with expected flame retardancy and enhanced toughness. However, thermal properties, such as thermal stability of these related thermosets were reduced due to the inferior intrinsic performance of these polymers.

In this work, a novel phosphorus-containing semi-aromatic polyester named poly[4,4′-bis(6-hydroxyhexyloxy)biphenyl 9,10-dihydro-10-[2,3-di(hydroxycarbonyl)propyl]-phosphaphenanthrene-10-oxide] (PBHDDP) was designed and synthesized, then utilized as a single-component additive combining toughening and flame-retardant effects for EP thermosets. Architecturally, PBHDDP contains a biphenyl group as rigid unit and six-methylene moiety as flexible spacer, and a bulky DOPO pendent as the flame-retardant group. The excellent combination of the rigid and flexible components made PBHDDP capable of toughening EP thermosets without sacrificing strength. Phase structure, thermal properties, flame retardancy and mechanical properties of the related EP thermosets were investigated systematically, and the potential no phase separation toughening mode-of-action was also proposed.

2. Experimental section

2.1. Materials

Diglycidyl ether of biphenol A (DGEBA, E-51, EEW = 184–200 g·eq^{-1}, viscosity at 25 °C = 7–18 Pa·s) was supplied by Lanxing Resin Co., Ltd. (Wuxi, China). 4,4′-Diaminodiphenyl methane (DDM, AR, 99.0%) was provided by Energy Chemical Co., Ltd. (Shanghai, China). PBHDDP was synthesized as illustrated in Scheme S1 in the supporting information. Molecular structures of DGEBA, DDM and PBHDDP were shown in Scheme 1.

2.2. Fabrication of the thermosets

All the thermosets were prepared according to the following identical experimental procedure. Initially, PBHDDP and DGEBA were mixed using mechanical stirrer in a glass flask at 80 °C under nitrogen (N_2) atmosphere to form a homogeneous mixture. A stoichiometric feed amount of DDM (DGEBA:DDM = 100:25, in weight) was added and stirred vigorously at 100 °C for 5 min, and then the mixture was degassed for 5 min in a vacuum oven at 100 °C. Subsequently, the above mixture was poured into a pre-heated Teflon mold and followed by a three-step curing procedure. The procedure was firstly carried out at 80 °C for 2 h, and then heated at 160 °C for 2 h; finally the procedure was performed at 180 °C for another 2 h. After curing, the samples were cooled naturally to room temperature. Neat EP was prepared via the same method as comparison. The thermoset with n weight part of PBHDDP per hundred EP resin (DGEBA + DDM) was denoted as EPn, where the number n denoted the weight part of PBHDDP per hundred EP resin (DGEBA + DDM). Formulations of samples were listed in Table 1 below.

Table 1
Formulation of the EP thermosets.

Samples	DGEBA (phr)	DDM (phr)	PBHDDP		P content
			phr	wt%	(wt%)
EP	80	20	0	0	0
EP1.0	80	20	1.0	0.99	0.04
EP2.5	80	20	2.5	2.44	0.11
EP5.0	80	20	5.0	4.76	0.21
EP10.0	80	20	10.0	9.09	0.40
EP12.5	80	20	12.5	11.11	0.49

2.3. Characterization

All the samples were dried for at least 24 h in vacuum at 80 °C prior to characterizations.

Morphologies of the fracture surfaces were observed by a field emission scanning electron microscope (FESEM, JEOL JSM 5900LV, Japan) at an activation voltage of 20 kV. The cryogenically fractured sample was etched with chloroform ($CHCl_3$) at room temperature for 12 h to observe the phase structure of the thermosets. Afterwards, the sample was coated with thin a layer of gold particles (about 100 Å). Energy dispersive X-ray spectrometer (EDX) was equipped for the elemental analysis in the surface scanning model.

Microstructures of the samples were determined by transmission electron microscopy (TEM, Tecnai G2F20 S-TWIN electron microscope, FEI, Holland), using stained ultrathin sections at an accelerated voltage of 200 kV. A representative piece of EP sheet was microtomed at room temperature using RMC cryoultramicrotome equipped with a diamond knife and mounted on Formvar-coated 200-mesh nickel grids. Ultrathin sections of ca. 70 to 80 nm in thickness were fabricated, then recovered on copper grids, and stained with a 0.5 wt% aqueous solution of ruthenium tetroxide (RuO_4) for 20 min.

Thermal stability was reflected via thermogravimetric analysis (TGA, 209 F1, NETZSCH, Germany) by heating from 40 to 700 °C at a heating rate of 10 °C min^{-1} under the N_2 flow of 50 mL·min^{-1} with 4–5 mg of samples.

Thermomechanical properties were determined using dynamic mechanical spectroscopy measurements (DMA, Q800, TA Instruments, USA) with a three-point bending configuration. The sample dimensions for DMA measurement were 30 × 10 × 4 mm^3. The testing was performed in dual cantilever mode at multi-frequencies of 1 Hz, the oscillation amplitude was fixed at 15.0 μm, with a heating rate of 5 °C min^{-1} from 0 to 240 °C. The dynamic storage modulus and tan δ curves were plotted as a function of temperature. The temperature at the maximum in tan δ curve was recorded as the T_α. The storage moduli at 50 °C was chosen as the glassy modulus (E_g).

Flame retardancy of thermosets was evaluated by limiting oxygen index (LOI) and Underwriter Laboratory 94 vertical burning tests (UL-94V). LOI tests were performed according to ASTM D2863, and measured on a HC-2C oxygen index meter (Jiangning Analysis Instrument Company, China) with a sheet dimension of 130 × 6.5 × 3 mm^3. UL-94V burning rating tests were conducted on a CZF-2 instrument (Jiangning Analysis Instrument Co., China) according to ATSM D3801 testing procedure with a sheet dimension of 130 × 13 × 3 mm^3. In the test, the samples were subjected to two 10 s flame application, and t_1 and t_2 were recorded as the two self-extinguish times. EP thermoset attains UL-94V-0 rating if each t_1 and t_2 of five samples don't exceed 10 s and the total burning time for five samples does not exceed 50 s at the same time without any dropping. Combustion behaviors of samples were recorded with a cone calorimeter device (Fire Testing Technology, UK) according to ISO 5660. Samples with the dimension of 100 × 100 × 3 mm^3 were exposed to a radiant cone at a heat flux of 35 kW·m^{-2}. All samples were placed on a holder filled with the mineral fiber blanket and mounted by frame without grid but padded with aluminum foil backing, leading to approximately 88 cm^2 of the sample surface being exposed to the external radiation from the cone heater. All the measurements were repeated three times and average data were reported.

Tensile properties were evaluated by using a universal testing machine (INSTRON F563-44, USA) according to ASTM D638 at 1 mm·min^{-1} cross-head speed. Flexural strength and modulus were measured by universal testing machine (CMT2000, China) using sample with regular dimensions loaded with a span of 32 mm at 2 mm·min^{-1} cross-head speed, according to ASTM D790. Unnotched Izod impact strength was conducted on a pendulum impact tester (ZBC1400-2, China) according to the ASTM D256.

3. Results and discussion

3.1. Morphology of EP thermosets

SEM and TEM were utilized to investigate the microstructure of the flame-retardant EP. As shown in Fig. 1(a) and (b), no holes were observed in high-magnification SEM image for EP12.5 etched in $CHCl_3$, neither could phase-separated morphology be observed in TEM image.

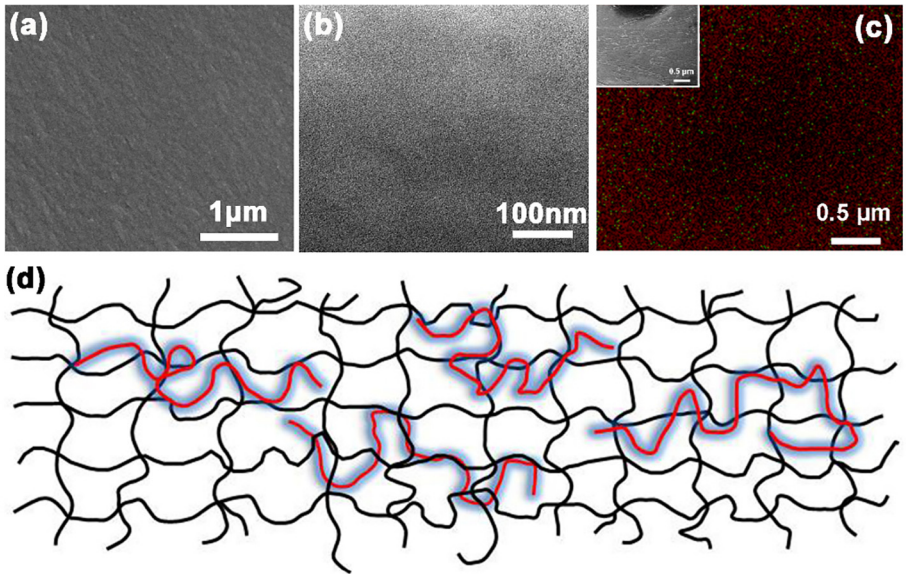

Fig. 1. (a) SEM micrograph of $CHCl_3$-etched fracture surface; (b) TEM image and (c) Merged EDX elements mapping image (C element in red signal and P in green signal) of EP12.5. (d) Feasible structural formation of the flame-retardant thermosets; the black networks denoted the cured epoxy networks and the red lines with blue border denoted the PBHDDP chains. (For interpretation of the references to colour in this figure legend, the reader is referred to the web version of this article.)

Table 2
Solubility parameters δ of different components.

	DGEBA prepolymer	DGEBA/DDM thermosets	PBHDDP
δ (MJ m^{-1})$^{1/2}$	20.50	20.95	20.93
V_A (cm^3 mol^{-1})	1749	704	1794
ρ_A (g cm^{-3})	1.16	1.18	1.25

Accordingly, no evidence for phase separation was found in the thermosets containing PBHDDP under the selected experimental condition, suggesting that PBHDDP was permeated into the EP network to form a semi-IPN structure, as illustrated in Fig. 1(d). Due to the absence of phase separation, all the resultant thermosets exhibited high transparency in visible light, as confirmed by their visual appearance and transmittance levels (see Fig. S4). SEM-EDX was applied to intuitively confirm the homogeneous desperation of PBHDDP in the matrix. As revealed in Fig. 1(c), PBHDDP was uniformly dispersed and distributed in EP matrix.

Generally, sufficient thermodynamic compatibility can avoid phase separation and the thermodynamic compatibility between different components in the blends can be elucidated in terms of the classic solubility parameters defined for different components [30]. Group contribution method is based on the hypothesis that the thermodynamic properties of the molecules can be estimated as the sum of each corresponding groups they are composed of [30]. In order to explore the affinity between PBHDDP and the EP network, the solubility parameters (δ) were calculated by Hansen group contribution method and the results were shown in Table 2. The corresponding calculation results were expressed by the following Eq. (1) [31,32]:

$$\delta = \sqrt{(\delta_d^2 + \delta_p^2 + \delta_h^2)} \tag{1}$$

δ_d, δ_p, and δ_h are calculated as following Eqs. (2)–(4)

$$\delta_d = \frac{\sum F_{d,i}}{V_m} \tag{2}$$

$$\delta_p = \frac{\sqrt{\sum F_{p,i}^2}}{V_m} \tag{3}$$

$$\delta_h = \sqrt{\frac{\sum E_{h,i}}{V_m}} \tag{4}$$

V_m is calculated as Eq. (5):

$$V_m = \frac{\rho}{M} \tag{5}$$

where, $F_{d,i}$ and $F_{p,i}$ are the group contributions for dispersive and polar forces, respectively; $E_{h,i}$ is the group contribution for the hydrogen bonding in the polymer, and V_m is the molar volume of the repeating unit at 298 K. ρ and M are the density measured at 25 °C and molar mass of the compound, respectively.

The proximity of solubility parameters is generally used to estimate the miscibility between different components. As shown in Table 2, the calculated δ value of PBHDDP was very close to the value of DGEBA prepolymer and the final thermosets, indicating that PBHDDP could be well dissolved in EP either before or after curing. It was plausible to propose that the PBHDDP was penetrated into the networks due to the good miscibility. The diffusion rate is the rate-determining step during the reaction-induced phase separation [33]. However, the strong interaction between PBHDDP and the EP thermosets, and the increased viscosity of the mixture considerably reduced the diffusion rate, thus making the system lack of sufficient time for phase separation before gelation.

3.2. Dynamic mechanical properties

Dynamic mechanical analysis (DMA) was utilized to further investigate the influence of PBHDDP on the thermal properties of the resultant thermosets. The plots of storage modulus (E') and loss factor (tan δ) versus temperature were presented in Fig. 2; and the corresponding data were listed in Table 3. The temperature at the maximum in the tan δ curve was recorded as the T_α (α relaxation), which was associated (but not equivalent) with the glass transition temperature (T_g) of the sample. It was noticed that no relaxation for PBHDDP was detected for all the flame-retardant EPs due to the relatively low content and feasible no phase separation of PBHDDP. In addition, the relaxation peaks of the modified thermosets were as narrow as that of the neat EP, indicating high interpenetration of PBHDDP in the matrices [27].

Interestingly, with low content, the highly dispersed PBHDDP acted as a reinforcing agent; whereas a higher PBHDDP content resulted in lower T_α, which agreed well with the variation trend of T_g recorded in DSC tests (Fig. S3). T_α values of these thermosets displayed a maximum at a content of 2.5 phr (2.44 wt%), following a decreasing trend with further increasing PBHDDP content, but still roughly equivalent to that of neat EP. This observation was explained by the two following effects arising simultaneously: molecular interlocking and plasticizing effects. Specifically, the slightly elevated T_α was ascribed to that the

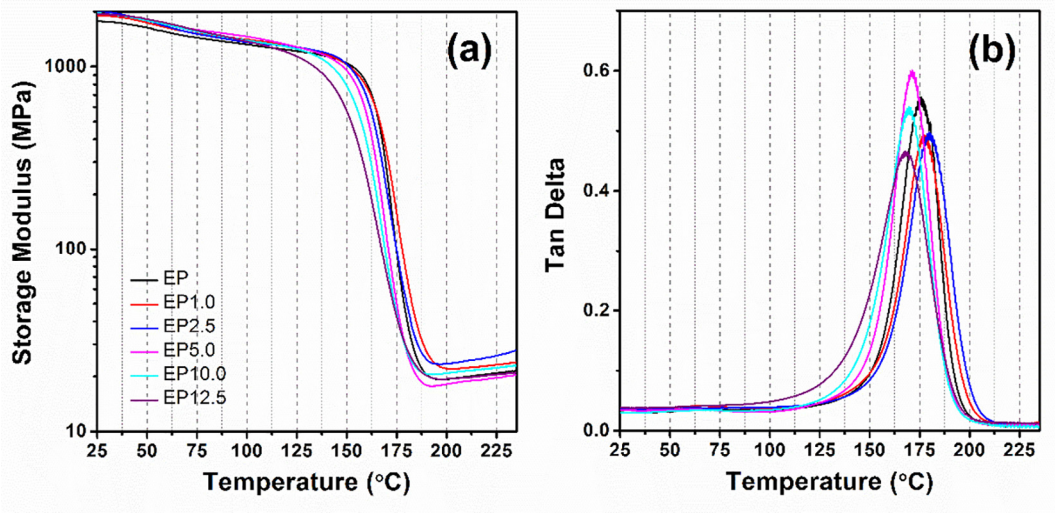

Fig. 2. (a) Storage modulus E', (b) loss tangent tan δ of neat EP and the flame-retardant thermosets.

Table 3
Thermal analysis data of PBHDDP, neat EP and the flame-retardant thermosets.

Samples	T_{d5} (°C)	T_{dmax} (°C)	Residue at 700 °C (wt%)	E_g (MPa)	T_α (°C)	T_g (°C)
PBHDDP	374.1	403.6	6.8	–	–	48
EP	371.4	386.7	15.8	1635	174	164
EP1.0	369.5	385.0	18.1	1738	176	167
EP2.5	369.6	386.3	18.5	1781	177	167
EP5.0	369.5	385.0	18.2	1799	171	164
EP10.0	368.8	385.1	18.6	1786	169	157
EP12.5	368.0	384.2	19.4	1815	168	157

incorporation of PBHDDP provided enhanced physical interactions (e.g. hydrogen bonding and entanglement constraints). On the one hand, these strong physical interactions acted as anchor points within the matrix, thus resulting in a strong confinement effect and restricting the cooperative motions of the EP network [27,34–36]. On the other hand, the flexible methylene chains of PBHDDP enhanced the mobility of their neighbouring network segments [10], thereby degrading the T_α of thermosets to a certain extent. The storage modulus, dependent on the rigidity of networks, was observed to slightly increase with an increasing content of PBHDDP, which was attributed to more rigid aromatic rings introduced into the network and physical interlocking between PBHDDP and the EP matrices.

By DSC, all the tested EP thermosets exhibited a single T_g (see Fig. S3), and it was in good agreement with the results of T_α obtained from DMA. The observation of single T_g between the constituent values for the amorphous components further confirmed the homogeneity of the thermosets. Mathematically, Fox equation can be used to predict the T_g of homogeneous blending systems [37]. The Fox equation describes the T_g of a polymer blend as Eq. (6):

$$\frac{1}{T_g} = \frac{w_1}{T_{g1}} + \frac{w_2}{T_{g2}} \tag{6}$$

where T_g is the predicted T_g of the blend; T_{g1} and T_{g2} are the T_gs of EP matrix and PBHDDP, respectively; w_1 and w_2 are the weight fractions of EP and PBHDDP, respectively. In Fig. 3, T_g data tested from DSC were plotted as a function of PBHDDP content. Calculated data from the Fox equation was also plotted for comparison. Obviously, the calculated ones were much lower than the experimental values. Since the Fox calculation extrapolated intermediate T_g values based on the weight fraction of two components, but ignoring the possible interactions between each other. Considering the intermolecular interactions among

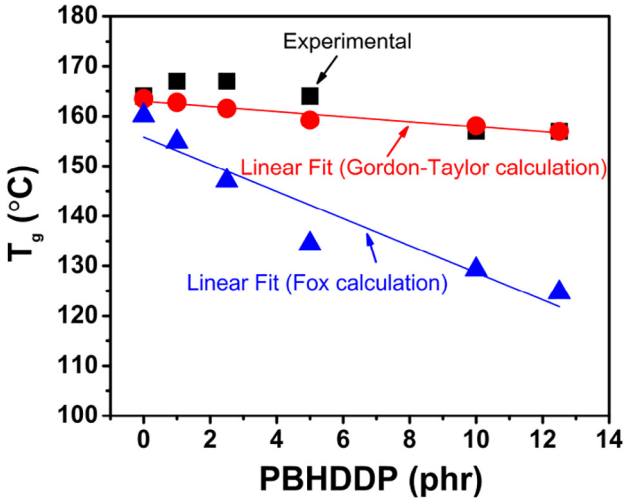

Fig. 3. Comparison of experimental and theoretical predicted values of T_g as a function of PBHDDP content in the thermosetting networks. Data-fitting lines based on the Fox equation and Gordon-Taylor equation (k = 0.51) were shown.

the components of polymer blend, Gordon-Taylor equation was employed to predict T_g of thermosets, by introducing the adjusting parameter, k [38,39]. A higher k value indicates an enhanced strength of intermolecular interactions (e.g. hydrogen bonding) [40,41]. The Gordon-Taylor equation is described as Eq. (7):

$$T_g = \frac{w_1 T_{g1} + k w_2 T_{g2}}{w_1 + k w_2} \tag{7}$$

Herein, for a given high k value of 0.51, the linear fitted Gordon-Taylor calculation showed good agreement with the experimental T_g values, especially for relatively higher contents of PBHDDP, while mildly underestimating T_g with PBHDDP content lower than 10 phr (9.09 wt%). These results indicated that the strong physical interaction played a critical role on maintaining T_g.

3.3. Thermal stability

TGA was carried out to investigate the thermal stability of the thermosets. TG-DTG profiles and the corresponding detailed data including the decomposition temperature at 5% weight loss (T_{d5}), the temperature at maximum weight loss rate (T_{dmax}) and the residues at 700 °C for samples under N_2 atmosphere were concluded in Fig. 4 and Table 3, respectively. The thermal decomposition process of all the thermosets containing PBHDDP presented similar degradation behavior to that of the neat EP reference, showing a single-step degradation progress referred to the DTG profile, without obvious changes in T_{d5} and T_{max}. Despite the decomposition residue of PBHDDP was extremely low, the incorporation of PBHDDP also led to relatively higher decomposition residues and lower maximum mass loss rates, showing positive role of PBHDDP on condensed flame-retardant activity.

3.4. Flame retardancy and combustion behavior

The flame retardancy of the thermosets was evaluated by Underwriter Laboratory-94 vertical burning test (UL-94V) and limiting oxygen index (LOI), and the results were summarized in Table 4. Obviously, despite the LOI value was 26.5%, neat EP was still considered as a flammable material that easily to be ignited and spread the flame. However, with increasing the PBHDDP content in the thermosets, the LOI value increased gradually. The thermoset containing 12.5 phr (11.11 wt%) PBHDDP showed a much higher LOI value of 34.0%. For neat EP, it displayed no rating (NR) in the UL-94V test: once ignited, it burned aggressively and could not self-extinguish, accompanying with flaming drips during combustion. It was noteworthy that no dripping phenomenon was observed during the UL-94V test for all samples containing PBHDDP. All the flame-retardant thermosets exhibited self-extinguishment, and the average burning time decreased with the increase of PBHDDP content. We also noticed that the burning flame was seemingly blew out by the pyrolytic gases from the charring surface, which was the so-called blowing-out effect. Similar phenomenon was also observed previously in other literatures [28,42].

Cone calorimetry is an effective method to evaluate the combustion behaviors of various polymer materials under a simulated real fire condition [43]. Various parameters, including time to ignition (TTI), peak of heat release rate (PHRR), total heat release (THR), time to peak of heat release rate (TTPHRR), average effective heat combustion (Av-EHC), maximum average heat rate emission (MAHRE), peak of smoke production rate (PSPR), total smoke production (TSP), and residues were summarized in Table 5. The corresponding curves of HRR and THR versus time were illustrated in Fig. 5. Unlike other conventional flame-retardant EP systems, the incorporation of PBHDDP led to higher TTIs rather than being ignited prematurely. For neat EP, once ignited, the HRR rapidly increased to the peak value (1191.5 kW m^{-2}) within 108 s. However, for EP12.5, the value was 802.9 kW m^{-2}, about 32.6% lower than that of neat EP. Similarly, with the increase of PBHDDP

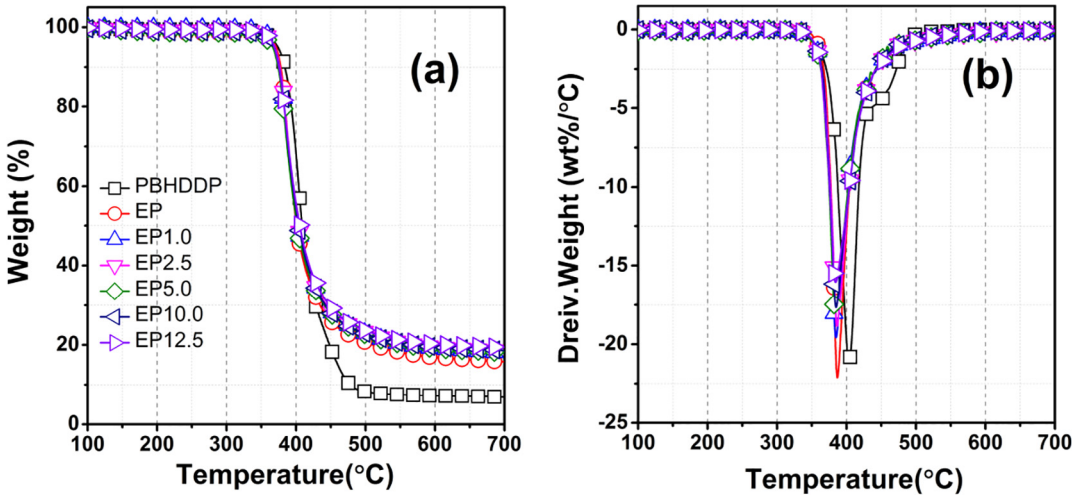

Fig. 4. (a) TG, (b) DTG curves of PBHDDP, the neat EP and flame-retardant thermosets in N_2 atmosphere.

Table 4
Detailed data of LOI and UL-94V tests of the testing samples.

Samples	LOI (%)	UL-94			
		Rating	t_1 (s)[b]	t_2 (s)[b]	Dripping
EP	26.5 ± 0.5	NR[a]	Burn-out	–	YES
EP1.0	28.0 ± 0.5	NR	32.9 ± 3.5	9.8 ± 1.9	NO
EP2.5	29.5 ± 0.5	V-1	21.9 ± 2.0	5.5 ± 2.3	NO
EP5.0	32.5 ± 0.5	V-1	11.1 ± 2.4	6.6 ± 3.4	NO
EP10.0	33.0 ± 0.5	V-1	6.2 ± 1.1	4.5 ± 2.7	NO
EP12.5	34.0 ± 0.5	V-0	4.7 ± 1.2	4.0 ± 1.3	NO

[a] No rating.
[b] Average burning time after the 10 s ignition.

Table 5
Cone calorimetric data of the testing samples.

	EP	EP5.0	EP10.0	EP12.5
TTI (s)	55 ± 3	68 ± 4	73 ± 3	72 ± 3
PHRR (kW m^{-2})	1191.5 ± 28.7	963.2 ± 9.9	909.6 ± 12.0	802.9 ± 21.7
THR (MJ m^{-2})	75.8 ± 6.4	66.7 ± 3.0	62.2 ± 4.6	61.3 ± 0.4
TTPHRR (s)	108 ± 3	133 ± 8	138 ± 3	138 ± 3
Av-EHC (MJ kg^{-1})	22.8 ± 1.1	22.3 ± 0.2	21.1 ± 0.9	20.2 ± 0.1
Residues (%)	14.5 ± 0.4	20.7 ± 2.4	26.2 ± 1.4	29.8 ± 1.2
MAHRE (kW m^{-2})	294.5 ± 7.6	274.1 ± 9.7	266.4 ± 12.4	231.2 ± 11.3
PSPR ($m^2 \cdot s^{-1}$)	0.32 ± 0.01	0.33 ± 0.03	0.31 ± 0.01	0.32 ± 0.01
TSP (m^2)	24.7 ± 0.4	23.1 ± 0.7	22.0 ± 0.8	24.6 ± 0.2
FIGRA[a] (kW m^{-2} s^{-1})	11.1	7.2	6.6	5.8

[a] FIGRA (fire growth rate) = PHRR/TTPHRR.

content, THR values of the flame-retardant thermosets decreased: the value for EP was 75.8 MJ m^{-2}; whereas the values for EP5.0, EP10.0 and EP12.5 were 66.7, 62.2 and 61.3 MJ m^{-2}, respectively. In addition, both the av-EHC and MAHRE values of all the flame-retardant thermosets exhibited remarkable reduction, indicating that PBHDDP effectively slowed down the flame propagation. Unlike the TGA results, all the flame-retardant thermosets showed much higher residues than that of neat EP after burning. The major benefit of DOPO-based compounds was that both gaseous and condensed phase activities worked on increasing the fire safety of materials [21,44]. On the one hand, the release of phosphorus-containing radicals such as PO· and PO_2·contributed to the extinction of the flame [45,46]. On the other hand, at the very beginning of combustion such as ignition stage, the majority of phosphorus-containing moieties were oxidized to phosphorus pentoxide (P_2O_5) and then hydrolysed to poly/ultra/pyrophosphoric acid(s) (HxPyOz), which played an important role on dehydrating and further charring processes, thus resulting in higher residues after cone calorimetry than TGA [16,47,48]. Raman spectroscopy and TG-FTIR test were carried out to further confirm the flame-retardant mode-of-action of PBHDDP in both condensed and gas phase; and the detailed results were supported in the supporting information. The lowered parameters such as PHRR, THR, av-EHC and MAHRE were partially ascribed to the increased burning residue, for the fact that an elevated burning residue meant less fuel generation during combustion. TSR and PSPR are two important parameters to evaluate the smoke release of the testing materials during combustion. Compared with neat EP, the addition of PBHDDP slightly decreased the TSP values but the PSPR values were almost unchanged, which was related to the compromised results of both enhanced gaseous and condensed flame-retardant activities [49]. The fire growth rate (FIGRA), defined as the value of PHRR divided TTPHRR, was calculated to evaluate the fire spread rate of the material. A lower FIGRA meant that the fire spreading was suppressed. For neat EP, the FIGRA was 11.1 kW m^{-2} s^{-1}; however, the FIGRA values decreased to 6.6 kW m^{-2} s^{-1} and 5.8 kW m^{-2} s^{-1} for EP10.0 and EP12.5, respectively, indicating more time to evacuate people in distress and/or reach for the fire extinguishers [15]. The improved flame retardancy of the resultant thermosets was mainly attributed to the well dispersion and distribution of PBHDDP (see Fig. 1d).

3.5. Mechanical properties

Generally, in most flame-retardant systems, high flame retardancy and excellent mechanical properties are usually mutually exclusive; the increase in one property often results in sacrificing the other. Accordingly, the influence of PBHDDP on mechanical properties, including tensile strength, impact strength, flexural strength and modulus of these resulting thermosets was investigated thoroughly, as summarized in Fig. 6. Without any modification, EP thermosets exhibited a high tensile strength (66.2 MPa) but low impact strength (12.4 kJ m^{-2}), as an inherently brittle material. Remarkably, the incorporation of a small amount of PBHDDP into the matrix led to simultaneous enhancements in both strength and toughness. The largest tensile strength among the flame-retardant samples was 86.6 MPa. It was believed that the superb tensile strength of PBHDDP (see Fig. S2) and the strong interfacial adhesion of the semi-IPN networks were responsible for the enhanced tensile properties. The increasing trend of flexural strength was consistent with tensile strength. The largest flexural strength of the

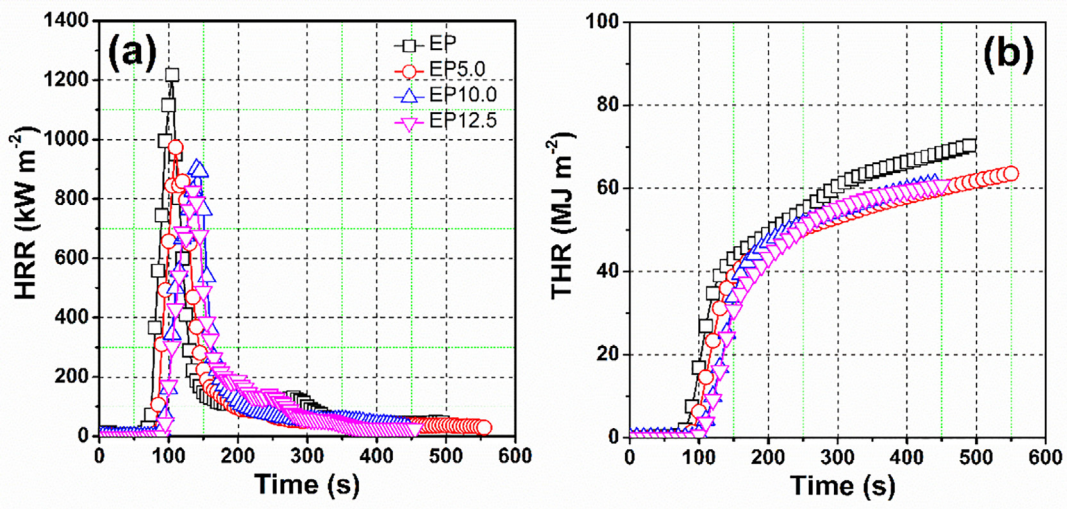

Fig. 5. HRR (a), THR (b) and mass (c) plots of the neat and flame-retardant EP thermosets obtained from cone calorimetry.

thermosets was 134 MPa, revealing 18.6% increments against neat EP. It is well-known that the flexural strength of EP thermosets is influenced by the interfacial adhesion between the modifiers and matrix [50], whereas the modulus is dependent on the rigidity of the networks. Thus the introduction of more rigid aromatic rings and the enhanced intermolecular interactions were the major reasons for the increase of flexural property.

As shown in Fig. 6(b), the addition of PBHDDP remarkably enhanced the impact strength of the resulting thermosets, indicating that the formed semi-IPN network indeed contributed to toughening the thermosets. With increasing the incorporation of PBHDDP, impact strength of the flame-retardant thermosets firstly exhibited considerable enhancement to reach the highest value of 30.9 kJ m^{-2} when the content of PBHDDP was 2.5 phr (2.44 wt%); then impact strength linearly decreased with further increasing the content of PBHDDP. The reduction in toughness was explained by the crowding effect of PBHDDP during the propagation of the EP network, thus leading to more internal defects in homogeneous system accounting for early failure of the material.

To the best of our knowledge, although tremendous efforts have been dedicated to developing high performance EP thermosets, and great progress has been made in some reported systems [29,51-53]; unfortunately, seldom works have been satisfactorily addressed the flammability and brittleness of EP at the same time by incorporation of a single compound. In this work, excellent comprehensive performance was achieved since the introduction of a relatively low content of PBHDDP, and the improved toughness and flame retardancy did not come at the cost of other important properties, such as modulus and thermal stability. As shown in Fig. 7, the highest increment in tensile strength, impact strength and LOI values of the flame-retardant EP thermosets in this work were compared with those collected from other relevant literatures. The comparison of these performances clearly suggested PBHDDP exhibited better performance in improving the comprehensive properties of the EP materials.

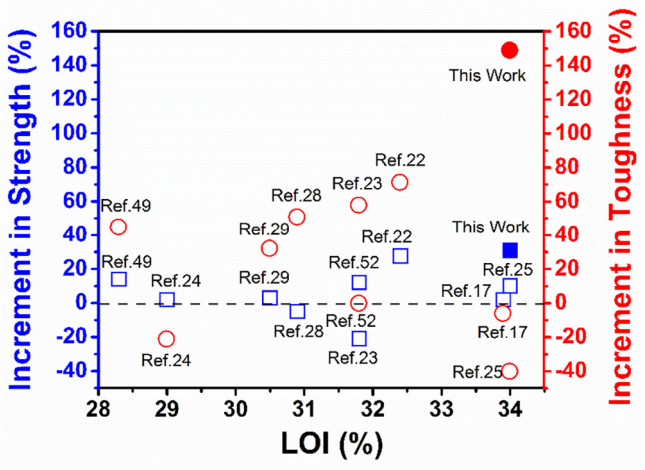

Fig. 7. Comparison for the highest increments in tensile strength, impact strength and LOI values of the flame-retardant EP thermosets between this work and other reported literatures.

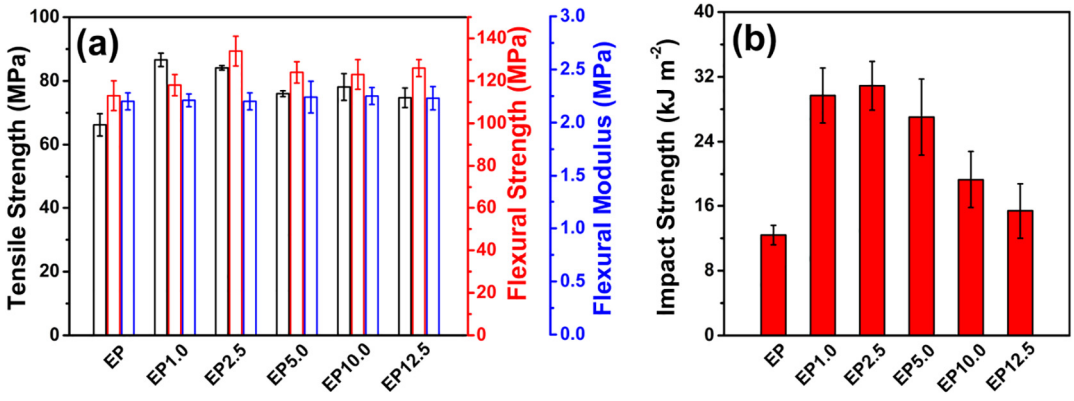

Fig. 6. Mechanical properties of the testing samples. (a) Tensile and flexural properties; (b) impact strength.

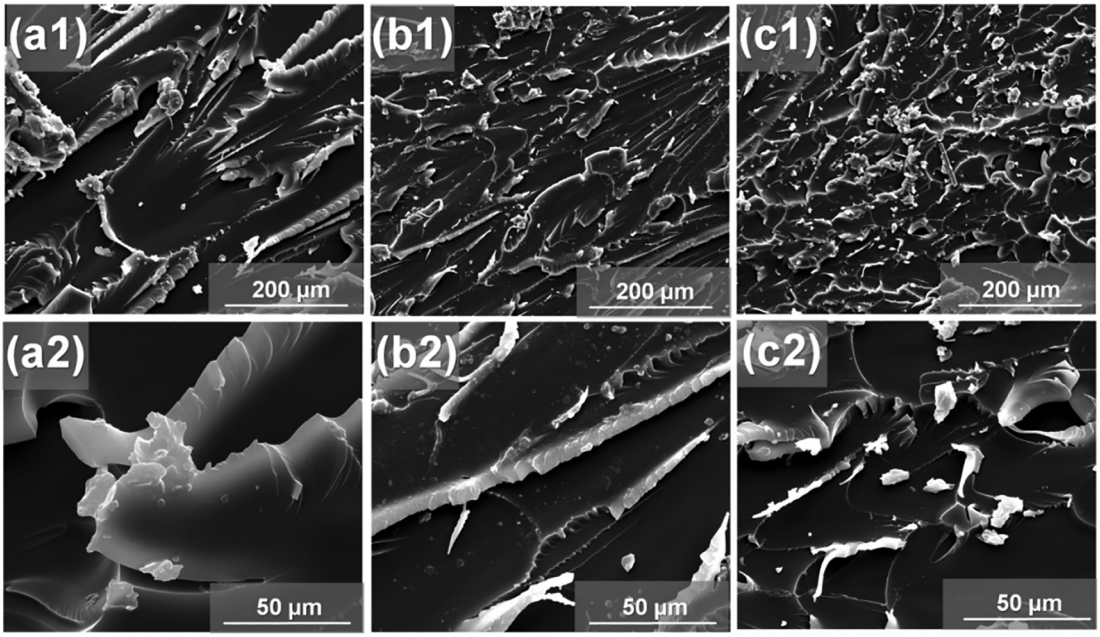

Fig. 8. SEM images of the fracture surfaces of samples: (a) neat EP, (b) EP2.5 and (c) EP10.0 at different magnification.

The overall improved mechanical properties were explained in terms of the rougher fracture surface morphologies. Hence, the fracture surfaces of samples after tensile test were examined using SEM to elucidate the toughening mode-of-action of PBHDDP on the thermosets, as shown in Fig. 8. It was well known that neat EP was extremely difficult to initiate shear deformation due to its high crosslinking density and rigid network [54]. As shown in Fig. 8(a), neat EP exhibited a characteristic brittle fracture surface with "radiation-like" patterns. The presence of a very few folds in addition to the smooth and featureless fracture surface of neat EP indicated the rapid crack propagation due to the lack of energy dissipation. Unlike neat EP, ductile fracture features were observed for the flame-retardant samples. For the representative fracture surface of EP2.5 (Fig. 8(b)), considerable increase of the ripples and folds was observed, indicating that the crack deflection prevented the rapid breakage of the material. The "dimple-like" structures were quite common in typical no phase separation toughened systems [9,28]. The relatively rougher fracture surface and the high amount of cracks meant the intricate fracture path and the enlarged fracture area, which were thought to certainly dissipate more energy, thereby leading to enhanced toughness. Plenty of EP debris, which arose from the defects in these cured thermosets, was observed on the fracture surface of EP10.0 (Fig. 8(c)). This phenomenon exhibited good agreement with the reduced tensile properties. The remarkable reinforcement and toughening effects of PBHDDP were relevant to the no phase separated morphology and PBHDDP's unique rigid and flexible molecular structure. On the one hand, the strongly adhering PBHDDP to the EP network allowed improving energy dissipation during the fracture event, and the polar phosphaphenanthrene group further enhanced the interaction between PBHDDP and the matrix [55]. On the other hand, the aliphatic chains of PBHDDP provided great flexibility of the network architecture, which meant it was more likely undergo uniform shear deformation and dissipated more fracture energy through intermolecular motions. Thus, PBHDDP acted in an energy absorption mode-of-action, described as "*in-situ* toughening" in previous literatures [9,56].

4. Conclusions

Challenges still remain to design and construct robust EP thermosets with concurrent enhancements on both flame retardancy and mechanical properties. Herein, a novel phosphorus-containing semi-aromatic polymer (PBHDDP) was successfully utilized as multi-functional component to endow EP thermosets with expected flame retardancy, desirable toughening and reinforcing performance simultaneously. Morphology analyses revealed that PBHDDP was highly distributed in EP matrix after curing, and typical no phase separated morphology was correspondingly formed in the thermosets, resulting in homogeneous distribution of the phosphorus and enhanced interfacial adhesion. Compared with neat EP, the resulting flame-retardant EP thermosets exhibited superior mechanical properties with 20.3% and 149.2% increase in tensile strength and impact strength with extremely low content (2.44 wt%) of PBHDDP, respectively. At the same time, a much better improvement in flame retardancy was also achieved, as evidenced by the enhanced anti-ignition and self-extinguishing performance showing in LOI and UL-94V tests, and the reduced combustion rate and heat release according to cone calorimetry results. With barely 0.49 wt% of phosphorus, LOI of the EP thermoset increased from 26.5% to 34.0% and UL-94V-0 rating was achieved. The reduced PHRR, THR, av-EHC, MAHRE and FIGRA values but prolonged TTI of the flame-retardant EP thermosets indicated that PBHDDP was effective in suppressing the combustion of EP thermosets. Meanwhile, these improvements were achieved without sacrificing the clarity, T_g and modulus of the resulting materials. Taking these features, PBHDDP/EP system holds attractive potential application in diverse areas.

Declaration of Competing Interest

The authors declare that they have no known competing financial interests or personal relationships that could have appeared to influence the work reported in this paper.

Acknowledgements

Financial supports by the National Natural Science Foundation of China (grant no. 51822304 and 51721091) and the Sichuan Province Youth Science and Technology Innovation Team (grant no. 2017TD0006) are sincerely acknowledged. The authors would also like to thank the Analysis and Testing Center of Sichuan University for the SEM and TEM measurements.

Appendix A. Supplementary data

Supplementary data to this article can be found online at https://doi.org/10.1016/j.cej.2019.122471.

References

[1] R. Auvergne, S. Caillol, G. David, B. Boutevin, J.P. Pascault, Biobased thermosetting epoxy: present and future, Chem. Rev. 114 (2014) 1082–1115.
[2] N. Domun, H. Hadavinia, T. Zhang, T. Sainsbury, G.H. Liaghat, S. Vahid, Improving the fracture toughness and the strength of epoxy using nanomaterials-a review of the current status, Nanoscale 7 (2015) 10294–10329.
[3] X. Shi, L. Chen, B. Liu, J. Long, Y. Xu, Y. Wang, Carbon fibers decorated by polyelectrolyte complexes toward their epoxy resin composites with high fire safety, Chin. J. Polym. Sci. 36 (2018) 1375–1384.
[4] A.J. Kinloch, Toughening epoxy adhesives to meet today's challenges, MRS Bull. 28 (2011) 445–448.
[5] L. Chen, S. Chai, K. Liu, N. Ning, J. Gao, Q. Liu, F. Chen, Q. Fu, Enhanced epoxy/silica composites mechanical properties by introducing graphene oxide to the interface, ACS Appl. Mater. Interfaces 4 (2012) 4398–4404.
[6] Z. Heng, Y. Chen, H. Zou, M. Liang, Simultaneously enhanced tensile strength and fracture toughness of epoxy resins by a poly(ethylene oxide)-block-carboxyl terminated butadiene-acrylonitrile rubber dilock copolymer, RSC Adv. 5 (2015) 42362–42368.
[7] R. Thomas, D. Yumei, H. Yuelong, Y. Le, P. Moldenaers, Y. Weimin, T. Czigany, S. Thomas, Miscibility, morphology, thermal, and mechanical properties of a DGEBA based epoxy resin toughened with a liquid rubber, Polymer 49 (2008) 278–294.
[8] Y. Zhang, W. Shi, F. Chen, C.C. Han, Dynamically asymmetric phase separation and morphological structure formation in the epoxy/polysulfone blends, Macromolecules 44 (2011) 7465–7472.
[9] T. Liu, Y. Nie, R. Chen, L. Zhang, Y. Meng, X. Li, Hyperbranched polyether as an all-purpose epoxy modifier: controlled synthesis and toughening mechanisms, J. Mater. Chem. 3 (2015) 1188–1198.
[10] M. Sharifi, C. Jang, C.F. Abrams, G.R. Palmese, Epoxy polymer networks with improved thermal and mechanical properties via controlled dispersion of reactive toughening agents, Macromolecules 48 (2015) 7495–7502.
[11] G. Yang, S.Y. Fu, J.P. Yang, Preparation and mechanical properties of modified epoxy resins with flexible diamines, Polymer 48 (2007) 302–310.
[12] K. Mimura, H. Ito, H. Fujioka, Toughening of epoxy resin modified with in situ polymerized thermoplastic polymers, Polymer 42 (2001) 9223–9233.
[13] K. Mimura, H. Ito, H. Fujioka, Improvement of thermal and mechanical properties by control of morphologies in PES-modified epoxy resins, Polymer 41 (2000) 4451–4459.
[14] D. Manjula Dhevi, S.N. Jaisankar, M. Pathak, Effect of new hyperbranched polyester of varying generations on toughening of epoxy resin through interpenetrating polymer networks using urethane linkages, Eur. Polym. J. 49 (2013) 3561–3572.
[15] Y. Tan, Z.B. Shao, X.F. Chen, J.W. Long, L. Chen, Y.Z. Wang, Novel multifunctional organic-Inorganic hybrid curing agent with high flame-retardant efficiency for epoxy resin, ACS Appl. Mater. Interfaces 7 (2015) 17919–17928.
[16] Y.J. Xu, J. Wang, Y. Tan, M. Qi, L. Chen, Y.-Z. Wang, A novel and feasible approach for one-pack flame-retardant epoxy resin with long pot life and fast curing, Chem. Eng. J. 337 (2018) 30–39.
[17] Y.Q. Shi, T. Fu, Y.J. Xu, D.F. Li, X.L. Wang, Y.Z. Wang, Novel phosphorus-containing halogen-free ionic liquid toward fire safety epoxy resin with well-balanced comprehensive performance, Chem. Eng. J. 354 (2018) 208–219.
[18] Y.J. Xu, L. Chen, W.H. Rao, M. Qi, D.M. Guo, W. Liao, Y.Z. Wang, Latent curing epoxy system with excellent thermal stability, flame retardance and dielectric property, Chem. Eng. J. 347 (2018) 223–232.
[19] Y. Zhang, B. Yu, B. Wang, K.M. Liew, L. Song, C. Wang, Y. Hu, Highly effective P-P synergy of a novel DOPO-based flame retardant for epoxy resin, Ind. Eng. Chem. Res. 56 (2017) 1245–1255.
[20] L. Qian, L. Ye, Y. Qiu, S. Qu, Thermal degradation behavior of the compound containing phosphaphenanthrene and phosphazene groups and its flame retardant mechanism on epoxy resin, Polymer 52 (2011) 5486–5493.
[21] M.M. Velencoso, A. Battig, J.C. Markwart, B. Schartel, F.R. Wurm, Molecular firefighting-how modern phosphorus chemistry can help solve the challenge of flame retardancy, Angew. Chem. 57 (2018) 10450–10467.
[22] G. Wang, Z. Nie, Synthesis of a novel phosphorus-containing epoxy curing agent and the thermal, mechanical and flame-retardant properties of the cured products, Polym. Degrad. Stab. 130 (2016) 143–154.
[23] H. Liu, X. Wang, D. Wu, Synthesis of a novel linear polyphosphazene-based epoxy resin and its application in halogen-free flame-resistant thermosetting systems, Polym. Degrad. Stab. 118 (2015) 45–58.
[24] G. Yang, W.H. Wu, Y.H. Wang, Y.H. Jiao, L.Y. Lu, H.Q. Qu, X.Y. Qin, Synthesis of a novel phosphazene-based flame retardant with active amine groups and its application in reducing the fire hazard of epoxy Resin, J. Hazard. Mater. 366 (2019) 78–87.
[25] J. Hu, J. Shan, D. Wen, X. Liu, J. Zhao, Z. Tong, Flame retardant, mechanical properties and curing kinetics of DOPO-based epoxy resins, Polym. Degrad. Stab. 109 (2014) 218–225.
[26] G. You, Z. Cheng, Y. Tang, H. He, Functional group effect on char formation, flame retardancy and mechanical properties of phosphonate-triazine-based compound as flame retardant in epoxy resin, Ind. Eng. Chem. Res. 54 (2015) 7309–7319.
[27] R.M. Perez, J.K.W. Sandler, V. Altstädt, T. Hoffmann, D. Pospiech, M. Ciesielski, M. Döring, U. Braun, A.I. Balabanovich, B. Schartel, Novel phosphorus-modified polysulfone as a combined flame retardant and toughness modifier for epoxy resins, Polymer 48 (2007) 778–790.
[28] C. Ma, S. Qiu, B. Yu, J. Wang, C. Wang, W. Zeng, Y. Hu, Economical and environment-friendly synthesis of a novel hyperbranched poly(aminomethylphosphine oxide-amine) as co-curing agent for simultaneous improvement of fire safety, glass transition temperature and toughness of epoxy resins, Chem. Eng. J. 322 (2017) 618–631.
[29] C. Ma, S. Qiu, J. Wang, H. Sheng, Y. Zhang, W. Hu, Y. Hu, Facile synthesis of a novel hyperbranched poly(urethane-phosphine oxide) as an effective modifier for epoxy resin, Polym. Degrad. Stab. 154 (2018) 157–169.
[30] C.M. Hansen, Hansen Solubility Parameters, Springer, New York, 2000.
[31] D.W. Van Krevelen, K. Te Nijenhuis, Cohesive Properties and Solubility, Properties of Polymers, fourth ed., Elsevier, 2009, pp. 189–227 Chapter 7.
[32] Q. Guan, L. Yuan, A. Gu, G. Liang, Fabrication of in situ nanofiber-reinforced molecular composites by nonequilibrium self-assembly, ACS Appl. Mater. Interfaces 10 (2018) 39293–39306.
[33] E. Petrie, Epoxy Adhesives Formulations, 2006.
[34] H. Feng, Z. Feng, H. Ruan, L. Shen, A high-resolution solid-state NMR study of the miscibility, morphology, and toughening mechanism of polystyrene with poly(2,6-dimethyl-1,4-phenylene oxide) blends, Macromolecules 25 (1992) 5981–5985.
[35] J. Wan, B. Gan, C. Li, J. Molina-Aldareguia, Z. Li, X. Wang, D.Y. Wang, A novel biobased epoxy resin with high mechanical stiffness and low flammability: synthesis, characterization and properties, J. Mater. Chem. A 3 (2015) 21907–21921.
[36] J. Ye, G. Liang, A. Gu, Z. Zhang, J. Han, L. Yuan, Novel phosphorus-containing hyperbranched polysiloxane and its high performance flame retardant cyanate ester resins, Polym. Degrad. Stab. 98 (2013) 597–608.
[37] D.G. Sycks, D.L. Safranski, N.B. Reddy, E. Sun, K. Gall, Tough semicrystalline thiolene photopolymers incorporating spiroacetal alkenes, Macromolecules 50 (2017).
[38] G. Bélorgey, M. Aubin, R.E. Prud'Homme, Studies of polyester/chlorinated poly (vinyl chloride) blends, Polymer 23 (1982) 1051–1056.
[39] M. Gordon, J.S. Taylor, Ideal copolymers and the second-order transitions of synthetic rubbers. I. Non-crystalline copolymers, J. Appl. Chem. 2 (1952) 493–500.
[40] I.M. Kalogeras, A. Stathopoulos, A. Vassilikoudova, W. Brostow, Nanoscale confinement effects on the relaxation dynamics in networks of diglycidyl ether of bisphenol-A and low-molecular-weight poly(ethylene oxide), J. Phys. Chem. B 111 (2007) 2774–2782.
[41] F.C. Chiu, K. Min, Miscibility, morphology and tensile properties of vinyl chloride polymer and poly (ε-caprolactone) blends, Polym. Int. 49 (2000) 223–234.
[42] W. Zhang, X. Li, R. Yang, Novel flame retardancy effects of DOPO-POSS on epoxy resins, Polym. Degrad. Stab. 96 (2011) 2167–2173.
[43] B. Schartel, T.R. Hull, Development of fire-retarded materials-Interpretation of cone calorimeter data, Fire Mater. 31 (2007) 327–354.
[44] M. Rakotomalala, S. Wagner, M. Döring, Recent developments in halogen free flame retardants for epoxy resins for electrical and electronic applications, Materials 3 (2010) 4300–4327.
[45] U. Braun, A.I. Balabanovich, B. Schartel, U. Knoll, J. Artner, M. Ciesielski, M. Döring, R. Perez, J.K. Sandler, V. Altstädt, Influence of the oxidation state of phosphorus on the decomposition and fire behaviour of flame-retarded epoxy resin composites, Polymer 47 (2006) 8495–8508.
[46] T. Mariappan, Y. Zhou, J. Hao, C.A. Wilkie, Influence of oxidation state of phosphorus on the thermal and flammability of polyurea and epoxy resin, Eur. Polym. J. 49 (2013) 3171–3180.
[47] D. Shen, Y.J. Xu, J.W. Long, X.H. Shi, L. Chen, Y.Z. Wang, Epoxy resin flame-retarded via a novel melamine-organophosphinic acid salt: thermal stability, flame retardance and pyrolysis behavior, J. Anal. Appl. Pyrol. 128 (2017) 54–63.
[48] R.K. Jian, Y.F. Ai, L. Xia, L.J. Zhao, H.B. Zhao, Single component phosphamide-based intumescent flame retardant with potential reactivity towards low flammability and smoke epoxy resins, J. Hazard. Mater. 371 (2019) 529–539.
[49] Y.X. Wei, C. Deng, H. Chen, L. Wan, W.C. Wei, Y.Z. Wang, Novel core-shell hybrid nanosphere towards the mechanical enhancement and fire retardance of polycarbonate, ACS Appl. Mater. Interfaces 10 (2018) 28036–28050.
[50] J. Jia, X. Sun, X. Lin, X. Shen, Y.W. Mai, J.K. Kim, Exceptional electrical conductivity and fracture resistance of 3D interconnected graphene foam/epoxy composites, ACS Nano 8 (2014) 5774–5783.
[51] Q. Luo, Y. Yuan, C. Dong, H. Huang, S. Liu, J. Zhao, Highly effective flame retardancy of a covel DPPA-based curing agent for DGEBA epoxy resin, Ind. Eng. Chem. Res. 55 (2016) 10880–10888.
[52] P. Wang, F. Yang, L. Li, Z. Cai, Flame retardancy and mechanical properties of epoxy thermosets modified with a novel DOPO-based oligomer, Polym. Degrad. Stab. 129 (2016) 156–167.
[53] C. Liu, T. Chen, C.H. Yuan, C.F. Song, Y. Chang, G.R. Chen, Y.T. Xu, L.Z. Dai, Modification of epoxy resin through the self-assembly of a surfactant-like multi-element flame retardant, J. Mater. Chem. A 4 (2016) 3462–3470.
[54] J. Liu, H.J. Sue, Z.J. Thompson, F.S. Bates, M. Dettloff, G. Jacob, N. Verghese, H. Pham, Effect of crosslink density on fracture behavior of model epoxies containing block copolymer nanoparticles, Polymer 50 (2009) 4683–4689.
[55] Y. Qiu, L. Qian, H. Feng, S. Jin, J. Hao, Toughening effect and flame-retardant behaviors of phosphaphenanthrene/phenylsiloxane bigroup macromolecules in epoxy thermoset, Macromolecules 51 (2018) 9992–10002.
[56] D. Zhang, D. Jia, Toughness and strength improvement of diglycidyl ether of bisphenol-A by low viscosity liquid hyperbranched epoxy resin, J. Appl. Polym. Sci. 101 (2010) 2504–2511.